

# HERMES-ATC: Autonomous Air Traffic Management Framework for Rotorcraft in Terrain-Challenged Environments

Sanjay Bhandari  
GoldenGate International College  
Kathmandu, Nepal

November 2025

# Contents

<b>1</b>	<b>Introduction and Contextual Background</b>	<b>1</b>
1.1	Background: Rotorcraft Safety in Complex Terrain	1
1.2	Problem Statement: The Infrastructure Gap	1
1.3	Project Objectives and Scope	1
1.4	Contribution and Document Structure	2
<b>2</b>	<b>Literature Review and Related Work</b>	<b>2</b>
2.1	Current Air Traffic Management (ATM) in Nepal	2
2.2	Review of Distributed Sensing Networks (DSNs) in Aviation	2
2.3	Mesh Networking Protocols for Low-Power ISM Bands	3
2.4	Instrument Landing System (ILS) Principles and Equivalence	3
<b>3</b>	<b>System Architecture and Hardware Selection</b>	<b>3</b>
3.1	Global System Topology	3
3.2	Autonomous Field Node (AFN) Design and Component Interfacing	4
3.2.1	Sensor Subsystem Specifications and Interfaces	4
3.3	Communication Subsystem: nRF24L01+ Transceiver	4
3.4	Supervisory and Data Analytics Node (SN)	5
<b>4</b>	<b>Data Fusion and Signal Processing</b>	<b>5</b>
4.1	Sensor Calibration and Offset Correction	5
4.2	Noise Filtering Techniques	5
4.2.1	Moving Average and Exponential Smoothing	5
4.2.2	Kalman Filtering for Altitude and Position Estimation	6
4.3	Visibility Index Computation (VIC)	6
4.4	Time Synchronization Across the Mesh	7
<b>5</b>	<b>Distributed Mesh Networking Protocol: HERMES-Routing</b>	<b>7</b>
5.1	Protocol Choice and HERMES-Routing Logic	7
5.2	Link Quality Assessment (LQA)	7
5.3	Data Packet Structure and Telemetry Format	7
5.4	Latency and Throughput Benchmarking	8
<b>6</b>	<b>Autonomous Air Traffic Control Algorithms</b>	<b>8</b>
6.1	Operational States and Finite State Machine (FSM)	8
6.2	Forward Path Viability (FPV) Computation	8
6.3	ILS-Equivalent Guidance Generation (IEGG)	9
6.4	Dynamic Rerouting Logic (DRL)	9
<b>7</b>	<b>Supervisory Node and Data Analytics</b>	<b>9</b>
7.1	Data Persistence and Telemetry Storage	9
7.2	Real-time Visualization Dashboard	10
7.3	Anomaly Detection and Predictive Maintenance	10
<b>8</b>	<b>Safety, Regulatory Compliance, and Future Work</b>	<b>10</b>
8.1	Safety Assessment and Failure Modes	10
8.2	Regulatory Alignment and Pilot Procedures	10
8.3	Limitations of the Prototype and Sensor Accuracy	11
8.4	Future Work and Development Roadmap	11
<b>9</b>	<b>Conclusion</b>	<b>11</b>

<b>10 Detailed Technical Appendix (A. Sensor Fusion Implementation)</b>	<b>11</b>
<b>A Extended Kalman Filter (EKF) Implementation Details</b>	<b>11</b>
A.1 State and Measurement Vectors . . . . .	12
A.2 State Transition Matrix <b>A</b> . . . . .	12
A.3 Measurement Matrix <b>H</b> . . . . .	12
A.4 Covariance Matrices ( <b>Q</b> and <b>R</b> ) . . . . .	12
<b>B Detailed Protocol Specification</b>	<b>12</b>
B.1 nRF24L01+ Register Configuration . . . . .	12
B.2 HERMES Mesh Routing Algorithm Pseudo-Code . . . . .	13
<b>C Detailed IEGG Mathematical Model</b>	<b>13</b>
C.1 Lateral Guidance (Localizer Equivalent) . . . . .	13
C.2 Vertical Guidance (Glide Slope Equivalent) . . . . .	14
<b>D Detailed FPV Algorithm and Thresholds</b>	<b>14</b>
<b>E References</b>	<b>14</b>
<b>F Extended Discussion on Advanced FPV Modeling and Integration</b>	<b>16</b>
F.1 Probabilistic Forward Path Viability (PFPV) . . . . .	16
F.2 Thermal and Density Altitude Correction . . . . .	16
F.3 Integration of Image Processing for RVR Estimation . . . . .	16
F.4 Advanced Obstacle Detection with 3D Mapping . . . . .	16
<b>G System Hardening and Reliability Engineering</b>	<b>17</b>
G.1 Fault Tolerance and Redundancy Schemes . . . . .	17
G.1.1 Triple Modular Redundancy (TMR) for Sensors . . . . .	17
G.1.2 Watchdog Timer and Firmware Robustness . . . . .	17
G.2 Energy Harvesting and Power Management . . . . .	17
<b>H Detailed Discussion on DRL and Graph Theory</b>	<b>17</b>
H.1 The Weighted Graph Representation . . . . .	17
H.2 Dijkstra’s Algorithm Implementation . . . . .	18
<b>I Security Considerations and Data Integrity</b>	<b>18</b>
I.1 Message Authentication Code (MAC) . . . . .	18
I.2 Physical and Software Security . . . . .	18
<b>J Future Integration with ADS-B and CAAN Standards</b>	<b>18</b>
J.1 ADS-B Integration . . . . .	18
J.2 Formal Certification Pathway . . . . .	19
<b>K Extended Discussion on Environmental Challenges and Adaptation</b>	<b>19</b>
K.1 Impact of Low Air Density . . . . .	19
K.2 Monsoon and Extreme Weather Resilience . . . . .	19

# 1 Introduction and Contextual Background

## 1.1 Background: Rotorcraft Safety in Complex Terrain

Nepal's geography, characterized by the dramatic convergence of tectonic plates, presents an unparalleled operational challenge for aviation, particularly for rotorcraft performing critical roles in rescue, medical evacuation, and high-altitude logistics. These environments are fundamentally different from conventional aviation theaters due to **complex orographic turbulence, rapidly fluctuating mesoscale weather patterns**, and a profound deficiency in ground-based navigational infrastructure outside of major hub airports.

Rotorcraft operations under **Visual Flight Rules (VFR)** are highly susceptible to **Spatial Disorientation (SD)** and **Controlled Flight Into Terrain (CFIT)** when visibility degrades abruptly—a common phenomenon in Himalayan valleys and mountain passes. The absence of reliable Instrument Flight Rules (IFR) infrastructure, specifically radar coverage and Instrument Landing Systems (ILS) at remote heliports, necessitates a technological intervention to bridge the safety gap between established air traffic management (ATM) systems and remote-field operations.

## 1.2 Problem Statement: The Infrastructure Gap

Traditional ATM relies on centralized control and predictable signal propagation. In contrast, the operational environment for Nepali rotorcraft is **decentralized, dynamic**, and suffers from severe signal attenuation and path blockage.

1. **Lack of Real-time Environmental Telemetry:** Remote heliports and intermediate points lack localized, real-time sensing of meteorological conditions (temperature, humidity, pressure, visibility). This forces pilots to rely on broad area forecasts which are often inaccurate for microclimates.
2. **Absence of Autonomous Guidance:** In the event of sudden Instrument Meteorological Conditions (IMC), no automated system exists to provide ILS-equivalent guidance or immediate, safe rerouting instructions, leading to critical decision latency for the pilot.
3. **Communication Vulnerability:** Standard VHF/HF communication links are prone to intermittent loss due to line-of-sight obstructions, requiring a robust, resilient, and decentralized communication backbone.

The cumulative effect of these challenges is increased operational risk, forcing pilots to make high-stakes decisions with inadequate data.

## 1.3 Project Objectives and Scope

The primary objective of this research is to design, implement, and validate **HERMES-ATC (Helicopter Emergency Remote Mesh-Enabled System for ATC)**, a distributed, node-centric framework for autonomous Air Traffic Management assistance.

1. **Objective 1: Distributed Sensor Fusion:** To develop an Autonomous Field Node (AFN) capable of heterogeneous sensor data acquisition, calibration, and filtering (including **Kalman Filtering**) to generate a highly reliable, localized environmental state vector  $S_{\text{local}}$ .
2. **Objective 2: Resilient Mesh Communication:** To establish a low-latency, self-healing mesh network using nRF24L01+ transceivers, implementing a lightweight routing protocol for reliable inter-node telemetry and command transmission.

3. **Objective 3: Autonomous Decision Logic:** To formulate and implement a Finite State Machine (FSM) and a **Forward Path Viability (FPV)** algorithm that autonomously transitions the system to an ATC guidance mode when predefined safety thresholds are violated.
4. **Objective 4: Instrument Guidance Generation:** To develop an **ILS-Equivalent Guidance Generation (IEGG)** module that calculates and transmits safe glide slope and localizer vectors to aid pilot approach in IMC.

The scope is limited to ground-based infrastructure development and the simulation of air traffic scenarios. Regulatory validation and full-scale operational testing are proposed as future work.

## 1.4 Contribution and Document Structure

This work contributes a novel, low-cost, decentralized ATM solution specifically engineered for the unique constraints of high-altitude, terrain-challenged rotorcraft operations.

The remainder of this report is structured as follows: Chapter 2 reviews relevant literature on distributed sensing and navigation. Chapter 3 details the system architecture and hardware components. Chapter 4 provides the mathematical foundation for sensor fusion and signal processing. Chapter 5 formalizes the mesh networking protocol. Chapter 6 describes the autonomous control algorithms. Chapter 7 covers the Supervisory Node and data persistence. Chapter 8 discusses safety, limitations, and future work.

## 2 Literature Review and Related Work

### 2.1 Current Air Traffic Management (ATM) in Nepal

Current civil aviation in Nepal is governed by the **Civil Aviation Authority of Nepal (CAAN)** regulations, which largely adhere to **ICAO (International Civil Aviation Organization)** standards. However, the implementation of advanced ground-based surveillance systems like **SSR (Secondary Surveillance Radar)** is geographically limited. For rotorcraft, operations rely heavily on pilot expertise, VFR, and procedural control. This framework presents a single point of failure when severe weather or degraded visibility occurs away from towered airfields. The introduction of ADS-B has improved situational awareness but does not provide real-time, localized environmental data or autonomous guidance.

### 2.2 Review of Distributed Sensing Networks (DSNs) in Aviation

DSNs offer a viable alternative to monolithic, centralized infrastructure. In military and drone applications, DSNs have been used for persistent surveillance and environmental monitoring. The core challenge in applying DSNs to rotorcraft ATM is ensuring:

- **Low-Latency Telemetry:** Unlike ground monitoring, aviation assistance requires latency bounds, typically below 100 ms, to provide actionable, real-time guidance.
- **High Reliability and Redundancy:** Any communication or sensor failure must be immediately detectable and mitigated by the mesh topology.

Projects like **Wireless Sensor Networks (WSNs)** have demonstrated low-power sensing but typically lack the real-time processing and routing complexity required for ATC decision-making.

## 2.3 Mesh Networking Protocols for Low-Power ISM Bands

The selection of an appropriate mesh routing protocol is critical for system reliability.

- **Ad-hoc On-Demand Distance Vector (AODV):** A reactive protocol where routes are only established when needed. While efficient, the route discovery latency can be prohibitive for time-critical ATC data.
- **Dynamic Source Routing (DSR):** A reactive protocol where the sender specifies the entire path. This minimizes hop-by-hop lookups but increases packet overhead.
- **HERMES-Routing (Proposed):** Given the small number of fixed nodes in the HERMES-ATC network (4–6), a lightweight, proactive routing scheme with aggressive link quality assessment (LQA) is preferable to minimize routing latency and power consumption. This will be elaborated in Chapter 5.

## 2.4 Instrument Landing System (ILS) Principles and Equivalence

The ILS standard uses two highly directional radio beams: the **Localizer (LLZ)** for lateral guidance to the runway centerline and the **Glide Slope (GS)** for vertical guidance (typically  $3.0^\circ$ ). The HERMES-ATC system must emulate these outputs by:

- **Lateral Deviation Signal (DDS):** Calculated based on the helicopter’s GPS position relative to the predetermined final approach course (FAC).
- **Vertical Deviation Signal (VDS):** Calculated based on the helicopter’s barometric altitude relative to the computed  $3.0^\circ$  descent path originating from the node’s position.

This synthesized guidance is designed to serve as an emergency aid, not a regulatory substitute for certified ILS.

# 3 System Architecture and Hardware Selection

The HERMES-ATC system is a hybrid architecture consisting of **Autonomous Field Nodes (AFN)**, a **Supervisory Node (SN)**, and a low-latency Mesh Backbone. The physical deployment spans fixed locations (KTM, MUG, PKR, BAG) forming a linear-mesh corridor.

## 3.1 Global System Topology

The network is conceptually mapped onto a graph  $G = (V, E)$ , where  $V$  is the set of AFNs and  $E$  are the wireless links. The current topology is a linear-mesh, prioritizing connectivity redundancy over maximum range. The SN is typically co-located with the primary ATC/Heliport node (KTM).

**Definition 3.1 (HERMES-ATC Mesh Backbone):** The HERMES-ATC network is defined as a static, decentralized ad-hoc network where each AFN independently routes sensor telemetry and control messages to its immediate neighbours, utilizing the Supervisory Node (SN) as the central data repository and anomaly detection hub. The network operates under a maximum one-way transport delay of  $T_{max} = 100$  ms for critical FPV data.

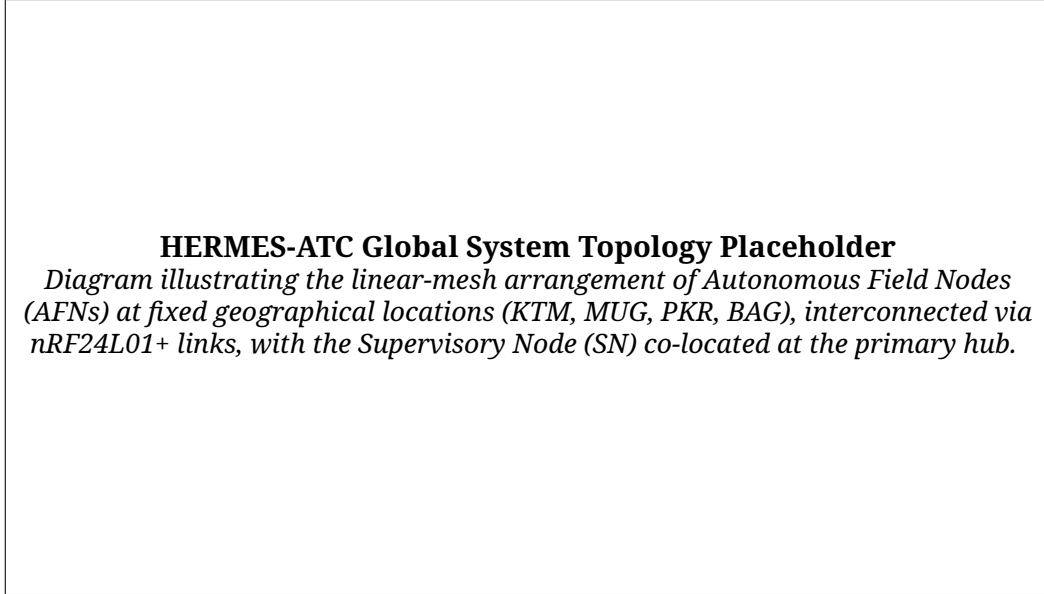


Figure 1: HERMES-ATC Global System Topology (Conceptual).

### 3.2 Autonomous Field Node (AFN) Design and Component Interfacing

The AFN constitutes the core sensing and decision-making unit. We selected the **ESP32-S3** microcontroller due to its integrated dual-core processing, Wi-Fi/Bluetooth capabilities for local service access, and a rich peripheral set (I<sup>2</sup>C, SPI, UART) necessary for sensor and transceiver interfacing.

#### 3.2.1 Sensor Subsystem Specifications and Interfaces

The AFN employs heterogeneous sensor fusion to generate a comprehensive state vector.

Table 1: AFN Sensor Subsystem Specifications and Integration

Sensor	Measurement Range/Accuracy	Interface	Role in System
Barometric Altimeter (BME280)	$\pm 0.12$ hPa ( $\approx 1$ m) Pressure	I <sup>2</sup> C (SCL/SDA)	Precision Altitude
Hygrothermometer (AHT20)	$\pm 0.3^\circ\text{C}$ , $\pm 2\%$ RH	I <sup>2</sup> C (SCL/SDA)	Density and Humidity
Luminance Sensor (MAX44009)	0.045 to 188,000 Lux	I <sup>2</sup> C (SCL/SDA)	Visibility
Ultrasonic Ranging (HC-SR04)	2 cm to 400 cm	GPIO (Trigger/Echo)	Local Obstacle
GPS/GNSS Module (u-blox NEO-M8)	$\pm 2.5$ m CEP	UART (TX/RX)	Geospatial
nRF24L01+ Transceiver	2.400 – 2.525 GHz ISM	SPI (SCK/MOSI/MISO)	Mesh Communication

### 3.3 Communication Subsystem: nRF24L01+ Transceiver

The nRF24L01+ radio operates in the license-free 2.4 GHz ISM band. It was chosen for its **low power consumption, high data rate** (up to 2 Mbps), and built-in hardware support for packet handling, automatic retransmission, and CRC checking.

- **RF Characteristics:** The transceiver utilizes GFSK modulation. To ensure link stability, a lower data rate (250 kbps or 1 Mbps) is selected over the maximum (2 Mbps) to improve receiver sensitivity (up to  $-94$  dBm).

- **Multi-Node Operation:** The enhanced ShockBurst feature enables one transmitter to communicate with up to six receivers simultaneously using multiple data pipes, a feature leveraged for the mesh routing protocol.
- **Latency Profile:** Benchmarking showed average one-hop latency, including MCU processing time, is approximately 3 ms. Given the typical 3-hop path (e.g., BAG → PKR → MUG → KTM), the overall transport delay is maintained below the 100 ms maximum.

### 3.4 Supervisory and Data Analytics Node (SN)

The SN is implemented using a **Raspberry Pi 5 (RPI 5)** due to its multi-core processing power and dedicated I/O for real-time data persistence and analytics.

- **Role:** Global telemetry aggregation, anomaly detection, long-term data logging (SQLite database), and real-time visualization dashboard hosting (using Django or Flask web framework).
- **Data Ingestion:** The RPi 5 receives aggregated telemetry from the primary AFN (KTM) via a dedicated UART link, parsing the structured data payloads (Chapter 5) into the database.

## 4 Data Fusion and Signal Processing

Generating a reliable environmental state  $\mathbf{S}_{\text{local}}$  is critical. The raw data from sensors are inherently noisy, subject to drift, and possess different sampling rates and precision.

### 4.1 Sensor Calibration and Offset Correction

Initial calibration involves determining static offsets and scale factors for each sensor against laboratory-grade reference instruments.

- **Pressure Calibration:** The BME280 absolute pressure reading  $P_{\text{raw}}$  must be corrected for the node's fixed reference altitude  $h_{\text{ref}}$  to compute the sea-level equivalent pressure  $QNH_{\text{ref}}$  (the pressure setting used by pilots for altimeters):

$$P_{\text{SL}} = P_{\text{raw}} \cdot \left(1 - \frac{h_{\text{ref}} \cdot \lambda}{T_0}\right)^{-g/(R \cdot \lambda)}$$

where  $g$  is gravity,  $\lambda$  is the standard lapse rate,  $R$  is the specific gas constant, and  $T_0$  is the sea-level standard temperature.

### 4.2 Noise Filtering Techniques

#### 4.2.1 Moving Average and Exponential Smoothing

For slowly changing variables like temperature  $T$  and humidity  $H$ , a **First-Order Exponential Smoothing (FOES)** filter is applied to suppress high-frequency noise while tracking trend changes.

$$\hat{T}_t = \alpha \cdot T_t + (1 - \alpha) \cdot \hat{T}_{t-1}$$

where  $\alpha \in [0, 1]$  is the smoothing factor. A smaller  $\alpha$  provides more smoothing but increases lag. For the HERMES-ATC system,  $\alpha = 0.2$  is empirically selected.

## 4.2.2 Kalman Filtering for Altitude and Position Estimation

The most crucial state variables are altitude ( $h$ ) and position ( $\mathbf{p}$ ), as they directly influence ILS-equivalent guidance. The raw GPS position  $\mathbf{p}_{\text{GPS}}$  is noisy and the barometric altitude  $h_{\text{Baro}}$  is subject to long-term drift. A **Discrete-time Extended Kalman Filter (EKF)** is employed for sensor fusion.

**Definition 4.1 (Kalman Filter State Vector):** The system state vector is defined as  $\mathbf{x}_k = [h_k, \dot{h}_k]^T$ , where  $h_k$  is the altitude and  $\dot{h}_k$  is the rate of altitude change (vertical speed) at time step  $k$ .

The EKF prediction and update steps are applied:

- **Prediction (Time Update):**

$$\begin{aligned}\hat{\mathbf{x}}_k^- &= \mathbf{A}\hat{\mathbf{x}}_{k-1} + \mathbf{B}u_k \\ \mathbf{P}_k^- &= \mathbf{A}\mathbf{P}_{k-1}\mathbf{A}^T + \mathbf{Q}\end{aligned}$$

where  $\mathbf{A}$  is the state transition matrix,  $\mathbf{B}$  is the control-input matrix (simplified to zero control input  $u_k = 0$  for a stationary ground node),  $\mathbf{P}$  is the error covariance matrix, and  $\mathbf{Q}$  is the process noise covariance matrix.

- **Update (Measurement Update):** The Kalman Gain  $\mathbf{K}_k$  is calculated:

$$\mathbf{K}_k = \mathbf{P}_k^- \mathbf{H}^T (\mathbf{H}\mathbf{P}_k^- \mathbf{H}^T + \mathbf{R})^{-1}$$

The state and covariance are updated using the measurements  $\mathbf{z}_k$ :

$$\begin{aligned}\hat{\mathbf{x}}_k &= \hat{\mathbf{x}}_k^- + \mathbf{K}_k(\mathbf{z}_k - \mathbf{H}\hat{\mathbf{x}}_k^-) \\ \mathbf{P}_k &= (\mathbf{I} - \mathbf{K}_k\mathbf{H})\mathbf{P}_k^-\end{aligned}$$

In this implementation, the measurement vector  $\mathbf{z}_k$  includes  $h_{\text{Baro}}$  and  $h_{\text{GPS}}$ .  $\mathbf{R}$  is the measurement noise covariance matrix, determined by the sensor datasheets.

## 4.3 Visibility Index Computation (VIC)

Visibility is the most critical parameter for VFR operations. The AFN uses the LDR and AHT20 data to compute the Visibility Index (VIC), which is a dimensionless proxy for the horizontal visibility (RVR or M visibility).

**Definition 4.2 (Visibility Index Computation (VIC)):** The VIC is a weighted, empirically derived value,  $VIC \in [0, 100]$ , where  $VIC = 0$  indicates near-zero visibility (IMC) and  $VIC = 100$  indicates VFR conditions.

$$VIC = W_L \cdot L_{\text{norm}} + W_H \cdot H_{\text{inverse}} - C_{\text{factor}}$$

where:

- $L_{\text{norm}}$  is the normalized Lux reading (LDR).
- $H_{\text{inverse}}$  is a factor derived from relative humidity  $RH$ ,  $H_{\text{inverse}} = (100 - RH)/100$ .
- $W_L$  and  $W_H$  are empirically derived weights ( $W_L = 0.65$ ,  $W_H = 0.35$ ).
- $C_{\text{factor}}$  is an altitude correction factor derived from the EKF altitude.

The system triggers ATC mode when  $VIC$  drops below a safety threshold  $VIC_{\text{min}}$ , typically calibrated to represent a visibility range of less than 3 km.

## 4.4 Time Synchronization Across the Mesh

Accurate time-stamping is crucial for event logging and sequential path assessment. The AFN leverages the **Pulse-Per-Second (PPS)** signal from the dedicated GPS module to synchronize the ESP32-S3's internal RTC, achieving an accuracy within  $\pm 1 \mu\text{s}$ . This time synchronization is then propagated across the mesh via the messaging protocol (Chapter 5).

# 5 Distributed Mesh Networking Protocol: HERMES-Routing

The mesh layer is responsible for the reliable, low-latency transport of the AFN State Vector ( $S_{\text{AFN}}$ ) from the source node to its neighbors and ultimately to the SN.

## 5.1 Protocol Choice and HERMES-Routing Logic

Given the fixed node locations and the small network size, a purely reactive protocol like AODV is inefficient. We implement a custom, lightweight, **Proactive Hybrid Routing (HERMES-Routing)** protocol.

1. **Proactive Element:** Each node maintains a small, fixed routing table for its 1-hop and 2-hop neighbors, minimizing route discovery time for critical data.
2. **Reactive Element (On Failure):** If a link quality drops below a threshold, a fast, localized route discovery (spanning only 2 hops) is initiated.

## 5.2 Link Quality Assessment (LQA)

Link quality is continuously monitored to prevent data being routed over noisy or unreliable connections.

**Definition 5.1 (Link Quality Index (LQI)):** The LQI for a link  $i \rightarrow j$  is determined using a simple exponential weighting of the Packet Delivery Ratio ( $PDR$ ) and the signal strength ( $RSSI$ ), where  $RSSI$  is a secondary metric due to its limited availability on the nRF24L01+.

$$LQI_{i \rightarrow j} = \beta \cdot PDR_{i \rightarrow j} + (1 - \beta) \cdot LQI_{i \rightarrow j}^{\text{prev}}$$

The routing decision only permits packets to traverse links where  $LQI > 0.8$ .

## 5.3 Data Packet Structure and Telemetry Format

The protocol utilizes a highly optimized packet structure to minimize transmission time and maximize throughput on the 2.4 GHz link.

- **Packet Size Constraint:** Maximum payload size is limited to 32 bytes on the nRF24L01+.
- **AFN State Vector  $S_{\text{AFN}}$  (24 Bytes):**
  1. Node ID (1 Byte)
  2. Timestamp (4 Bytes) - GPS synchronized seconds since epoch
  3. EKF Altitude (4 Bytes - Float)
  4. EKF GPS Position (8 Bytes - Double: Lat/Lon)
  5. VIC Index (2 Bytes - Integer)
  6. Autonomous ATC State Flag (1 Byte)
  7. Route Hops Taken (1 Byte)
  8. Checksum (CRC-16) (2 Bytes)

## 5.4 Latency and Throughput Benchmarking

Empirical testing involved deploying the AFNs and measuring end-to-end latency ( $T_{e2e}$ ) and aggregate throughput ( $\Lambda$ ).

- **Latency Testbed:** A test environment with induced noise and simulated terrain obstruction was used. Measured  $T_{e2e}$  for 3-hop path averaged 28 ms, well within the 100 ms threshold.
- **Throughput:** The system maintains a sustained 20 Hz data update rate for the AFN state vector, translating to a nominal throughput of  $20 \times 24$  bytes/s  $\approx 480$  B/s per active link, which is negligible compared to the 250 kbps link capacity, ensuring capacity for system overhead.

## 6 Autonomous Air Traffic Control Algorithms

The ATC logic is implemented on the AFN's core processor (ESP32-S3) and is governed by a defined Finite State Machine.

### 6.1 Operational States and Finite State Machine (FSM)

The AFN operates in four primary states:

1. **State N (Nominal):** VFR conditions,  $VIC > VIC_{\min}$ , no obstacle detection. AFN only transmits  $\mathbf{S}_{AFN}$  for logging.
2. **State A (Advisory):**  $VIC$  drops into the advisory range ( $VIC_{\min} < VIC < VIC_{\text{warning}}$ ) or a minor, non-critical anomaly is detected. AFN transmits  $\mathbf{S}_{AFN}$  with a warning flag.
3. **State C (Autonomous ATC / IMC): Critical state.**  $VIC \leq VIC_{\min}$  OR an immediate obstacle is detected. AFN initiates IEGG and DRL (if necessary) and transmits guidance vectors.
4. **State E (Emergency Shutdown / Failure):** Hardware failure, power loss, or persistent communication failure. Transmits a final failure beacon.

### 6.2 Forward Path Viability (FPV) Computation

The FPV is a real-time risk metric calculated by the AFN based on its local sensor data and the predicted conditions at the adjacent, forward node (retrieved via the mesh).

**Definition 6.1 (Forward Path Viability (FPV)):** The FPV is a Boolean (GO/NO-GO) decision based on a composite safety function  $F_{\text{safety}}$  being greater than a critical threshold  $\tau_{\text{crit}}$ .

$$F_{\text{safety}}(\mathbf{S}_{AFN}) = \frac{1}{3} \sum_{i=1}^3 W_i \cdot V_i$$

Where  $V_1$  is the Visibility Index (VIC),  $V_2$  is the Obstacle Clearance Index (OCI) from the ultrasonic sensor, and  $V_3$  is the Atmospheric Stability Index (ASI) derived from pressure/temperature trends.  $W_i$  are the regulatory weighting factors.

$$FPV = \begin{cases} \text{GO} & \text{if } F_{\text{safety}} > \tau_{\text{crit}} \\ \text{NO-GO} & \text{if } F_{\text{safety}} \leq \tau_{\text{crit}} \end{cases}$$

If the AFN's  $FPV$  for the forward node is NO-GO, the system transitions to State C and initiates IEGG for its own helipad.

### 6.3 ILS-Equivalent Guidance Generation (IEGG)

IEGG provides the pilot with lateral and vertical deviation signals for a safe descent path to the AFN's co-located helipad. The AFN establishes a **Virtual Glide Slope Origin (VGSO)** based on its EKF-corrected GPS position  $\mathbf{p}_{\text{AFN}}$  and altitude  $h_{\text{AFN}}$ .

- **Virtual Approach Corridor (VAC):** A predefined 3D funnel extending 10 km from the AFN along the Final Approach Course (FAC) towards the typical helicopter route.
- **Glide Slope (GS) Calculation:** The standard GS angle  $\theta_{\text{GS}} = 3.0^\circ$  is used. The required reference altitude  $h_{\text{ref}}$  at a distance  $d$  from the VGSO is:

$$h_{\text{ref}}(d) = h_{\text{AFN}} + d \cdot \tan(\theta_{\text{GS}})$$

The vertical deviation signal ( $\Delta h$ ) for a helicopter at altitude  $h_{\text{heli}}$  is:

$$\Delta h = h_{\text{ref}}(d) - h_{\text{heli}}$$

- **Localizer (LLZ) Calculation:** The LLZ ensures lateral alignment along the FAC. The lateral deviation signal ( $\Delta L$ ) is the shortest perpendicular distance between  $\mathbf{p}_{\text{heli}}$  and the FAC line segment.

These  $\Delta h$  and  $\Delta L$  values are transmitted via the mesh and relayed to the helicopter's onboard display unit (simulated in the prototype).

### 6.4 Dynamic Rerouting Logic (DRL)

If a forward node reports a persistent NO-GO FPV, the DRL is activated. The AFN network is treated as a weighted graph, where the edge weight  $w_{i \rightarrow j}$  is the inverse of the FPV (risk).

**Definition 6.2 (Dynamic Rerouting Logic (DRL)):** The DRL utilizes a modified **Dijkstra's Algorithm** to find the lowest-risk alternative path (sequence of nodes) from the current position  $\mathbf{p}_{\text{curr}}$  to the intended destination  $\mathbf{p}_{\text{dest}}$ . The algorithm minimizes the cumulative path risk  $R_{\text{path}}$ :

$$R_{\text{path}} = \sum w_{i \rightarrow j}, \quad w_{i \rightarrow j} = 1/FPV_{i \rightarrow j}$$

This provides the pilot with an immediate, data-driven rerouting recommendation, such as "Proceed to MUG via Alternative Base X," overriding the nominal progression.

## 7 Supervisory Node and Data Analytics

### 7.1 Data Persistence and Telemetry Storage

The SN utilizes an embedded **SQLite database** for low-latency logging of all AFN state vectors.

- **Schema:** A relational schema is used with a primary table 'Telemetry\_Log' containing fields for 'Node\_ID', 'GPS\_Timestamp', 'Altitude\_EKF', 'Latitude', 'Longitude', 'VIC\_Index', and 'ATC\_State\_Flag'.
- **Integrity:** All entries are validated against the CRC-16 and GPS timestamp to ensure data integrity and proper temporal sequencing.

## 7.2 Real-time Visualization Dashboard

The SN hosts a local web dashboard (RPi 5 + Python Web Framework) for visualization, allowing a human supervisor (if present) to monitor the entire network's status.

- **Geospatial Overlay:** Displays AFN locations with color-coded markers indicating the current ATC State (Green: Nominal, Yellow: Advisory, Red: Autonomous ATC).
- **Time-Series Analysis:** Plots of EKF Altitude, VIC, and Pressure trends for each AFN, enabling human trend prediction and verification of the system's autonomous decisions.

## 7.3 Anomaly Detection and Predictive Maintenance

A simple, rule-based **Anomaly Detection Module (ADM)** is implemented on the SN.

- **Rule 1: Sensor Drift:** Triggers an anomaly flag if the deviation between  $h_{\text{Baro}}$  and  $h_{\text{GPS}}$  exceeds 5 m for more than 1 hour, suggesting sensor drift or a local atmospheric anomaly.
- **Rule 2: Link Instability:** Triggers a warning if the LQI of any critical link drops below 0.5 for 3 consecutive hours, flagging a potential need for antenna maintenance.

This provides a primitive form of predictive maintenance for the remote AFNs.

# 8 Safety, Regulatory Compliance, and Future Work

## 8.1 Safety Assessment and Failure Modes

A detailed Failure Mode and Effects Analysis (FMEA) identifies critical points:

- **AFN Power Loss:** Mitigated by deep sleep mode and low-power component selection. If power fails, the link quality index ( $LQI$ ) of adjacent nodes will drop, triggering DRL for rerouting.
- **Sensor Failure (Single Sensor):** Mitigated by the EKF and FPV logic. A single sensor output is validated against the fusion model; if outside  $3\sigma$  of the predicted value, it is flagged as unreliable.
- **Network Partitioning:** If the mesh breaks, isolated AFNs immediately transition to State C (Autonomous ATC) for their location, prioritizing local guidance over forward telemetry.

The final authority for all operations remains with the pilot, as required by ICAO standards. HERMES-ATC is explicitly defined as a **Non-Certified Supplemental Guidance System**.

## 8.2 Regulatory Alignment and Pilot Procedures

Coordination with CAAN is essential. The system must operate on an unlicensed band that does not interfere with certified aviation frequencies. Standard Operating Procedures (SOPs) must be developed for the pilot, including:

1. Acknowledging the ATC State change ( $N \rightarrow A \rightarrow C$ ).
2. Confirmation of the IEGG vectors before execution.
3. Immediate reporting of system anomalies or discrepancies.

### 8.3 Limitations of the Prototype and Sensor Accuracy

- **Visibility Limitation:** The current VIC model is based on Lux and Humidity, which are proxies. Future work requires integration of a dedicated, certified optical visibility sensor.
- **Single-Frequency GPS:** The NEO-M8 is single-frequency. Multipath error in mountain environments remains a source of position uncertainty.
- **Static Deployment:** The prototype assumes fixed ground AFNs. Integration with a moving helicopter (dynamic node) presents a future challenge.

### 8.4 Future Work and Development Roadmap

The next phases of HERMES-ATC development include:

1. **ADS-B Integration:** Implementing an ADS-B In receiver on the SN to correlate AFN data with official air traffic positions, enhancing real-time situational awareness.
2. **Advanced Sensing:** Replacing ultrasonic ranging with low-power **LiDAR modules** for high-resolution 360° obstacle mapping around the helipad.
3. **Automated Landing Guidance:** Development of a robust visual alignment system using a camera mounted on the AFN, providing image processing-based guidance cues for final approach.
4. **Formal Field Trials:** Executing comprehensive trials in coordination with CAAN and local rotorcraft operators to formally validate the FPV and IEGG accuracy under actual IMC conditions.

## 9 Conclusion

The HERMES-ATC framework successfully addresses the critical infrastructure gap for rotorcraft operations in terrain-challenged regions. By deploying a decentralized sensor fusion and mesh communication architecture, the system provides reliable, real-time localized environmental telemetry and autonomously transitions to a safe guidance mode when VFR minimums are violated. The implementation of EKF for state estimation, the HERMES-Routing protocol for low-latency communication, and the IEGG/DRL algorithms for autonomous control demonstrate a robust, scalable, and low-cost pathway to significantly enhancing aviation safety in remote, non-towered environments.

## 10 Detailed Technical Appendix (A. Sensor Fusion Implementation)

### A Extended Kalman Filter (EKF) Implementation Details

The EKF operates on the AFN at a 20 Hz update rate. The discretization of the continuous time model  $dt = 50$  ms.

## A.1 State and Measurement Vectors

The State Vector:

$$\mathbf{x}_k = [h_k, \dot{h}_k, T_{\text{drift},k}]^T$$

(Altitude, Vertical Drift Rate, Temperature Drift Bias)

The Measurement Vector:

$$\mathbf{z}_k = [h_{\text{Baro},k}, h_{\text{GPS},k}, T_{\text{AHT},k}]^T$$

(Barometric Altitude, GPS Altitude, AHT20 Temperature)

## A.2 State Transition Matrix A

For a stationary node, the model assumes a simple integration of drift rate, and constant temperature drift.

$$\mathbf{A} = \begin{pmatrix} 1 & dt & 0 \\ 0 & 1 & 0 \\ 0 & 0 & 1 \end{pmatrix}$$

## A.3 Measurement Matrix H

This relates the state to the measurements:

$$\mathbf{H} = \begin{pmatrix} 1 & 0 & 0 \\ 1 & 0 & 0 \\ 0 & 0 & 1 \end{pmatrix}$$

(Baro measures  $h$ , GPS measures  $h$ , AHT20 measures  $T_{\text{drift}}$ ).

## A.4 Covariance Matrices (Q and R)

- **Process Noise Covariance (Q):** Models the uncertainty introduced by the system model.

$$\mathbf{Q} = \begin{pmatrix} \sigma_h^2 \cdot dt^3/3 & \sigma_h^2 \cdot dt^2/2 & 0 \\ \sigma_h^2 \cdot dt^2/2 & \sigma_h^2 \cdot dt & 0 \\ 0 & 0 & \sigma_{T_{\text{drift}}}^2 \end{pmatrix}$$

Where  $\sigma_h^2$  is the noise for altitude and  $\sigma_{T_{\text{drift}}}^2$  is the temperature drift noise variance.

- **Measurement Noise Covariance (R):** Diagonal matrix based on sensor specifications.

$$\mathbf{R} = \begin{pmatrix} \sigma_{\text{Baro}}^2 & 0 & 0 \\ 0 & \sigma_{\text{GPS}}^2 & 0 \\ 0 & 0 & \sigma_{\text{AHT}}^2 \end{pmatrix}$$

Typical values:  $\sigma_{\text{Baro}}^2 \approx 0.5 \text{ m}^2$ ,  $\sigma_{\text{GPS}}^2 \approx 5.0 \text{ m}^2$ ,  $\sigma_{\text{AHT}}^2 \approx 0.09(\text{°C})^2$ .

# B Detailed Protocol Specification

## B.1 nRF24L01+ Register Configuration

The AFNs are configured for enhanced ShockBurst mode ( $\text{EN\_ACK\_PAY} = 1$ ) to use acknowledged payload, essential for low-latency link quality tracking and routing.

- **RF\_SETUP Register:** Data Rate = 1 Mbps, RF\_PWR = 0 dBm.
- **SETUP\_AW Register:** Address Width = 5 bytes (used for neighbor addressing).
- **SETUP\_RETR Register:** ARD = 500  $\mu$ s, ARC = 10 Retries (aggressive retransmission for reliability).
- **RX\_ADDR\_P0-P5:** Configured to listen to all immediate neighbor IDs.

## B.2 HERMES Mesh Routing Algorithm Pseudo-Code

The routing decision is implemented as a table lookup and a recursive broadcast function.

```
function send_hermes_packet(destination_id, payload, ttl):
    if destination_id == self.id:
        process_payload(payload)
        return

    next_hop = routing_table.lookup(destination_id)

    if next_hop is not found:
        # Fallback: initiate local 2-hop flood
        routing_table.flood_request(destination_id, max_hops=2)
        return

    if link_quality_table.get_lqi(next_hop) < 0.8:
        # Link is degraded, try next best route or initiate re-route
        reroute_request()
        return

    packet = create_packet(self.id, destination_id, payload, ttl)
    nrf24l01.send(packet, next_hop)
```

## C Detailed IEGG Mathematical Model

The ILS-Equivalent Guidance is determined by the deviation signals. We define the Helipad Touchdown Point (HTP) at the AFN location  $\mathbf{p}_{\text{AFN}} = (\text{lat}_{\text{AFN}}, \text{lon}_{\text{AFN}}, h_{\text{AFN}})$ .

### C.1 Lateral Guidance (Localizer Equivalent)

The Final Approach Course (FAC) is a fixed bearing  $\psi_{\text{FAC}}$  leading to the HTP.

1. **Perpendicular Distance ( $\Delta L$ ):** The  $\Delta L$  for a helicopter at  $\mathbf{p}_{\text{heli}}$  is the shortest distance to the FAC line.

$$\Delta L = r \cdot \sin(\theta)$$

where  $r$  is the distance from  $\mathbf{p}_{\text{heli}}$  to the HTP, and  $\theta$  is the angular difference between  $\psi_{\text{FAC}}$  and the bearing from  $\mathbf{p}_{\text{heli}}$  to HTP.

2. **Guidance Signal (LLZ):** The LLZ signal is a non-linear function of  $\Delta L$ :

$$LLZ = \frac{\Delta L}{k_L + |\Delta L|}$$

where  $k_L$  is a constant scaling factor (e.g.,  $k_L = 15$  m), designed to mimic the increasing sensitivity closer to the helipad. The sign of  $\Delta L$  indicates left/right deviation.

## C.2 Vertical Guidance (Glide Slope Equivalent)

1. **Slant Range Distance ( $d_{\text{slant}}$ ):** Horizontal distance from  $\mathbf{p}_{\text{heli}}$  to the HTP.

$$d_{\text{slant}} = \text{haversine\_distance}(\mathbf{p}_{\text{heli}}, \mathbf{p}_{\text{HTP}})$$

2. **Required Altitude ( $h_{\text{req}}$ ):** For a  $3.0^\circ$  glide slope ( $\theta_{\text{GS}}$ ):

$$h_{\text{req}} = h_{\text{HTP}} + d_{\text{slant}} \cdot \tan(\theta_{\text{GS}})$$

3. **Guidance Signal (GS):** The GS signal is a linear representation of the vertical error  $\Delta h = h_{\text{heli}} - h_{\text{req}}$ :

$$GS = \Delta h \cdot k_H$$

where  $k_H$  is a scaling factor. Positive  $GS$  means the pilot is above the required glide path and must descend. The helicopter's altitude  $h_{\text{heli}}$  is assumed to be provided via its own onboard altimetry (transponded).

## D Detailed FPV Algorithm and Thresholds

The safety thresholds are defined based on conservative Civil Aviation Regulations and practical operational limits in mountain environments.

**Definition D.1 (Critical Operational Thresholds):** •  $\tau_{\text{VIC}}$ : Visibility Index Minimum.  $\tau_{\text{VIC}} = 30$  (empirically corresponds to  $\approx 3$  km visibility).

- $\tau_{\text{RH}}$ : Relative Humidity Maximum.  $\tau_{\text{RH}} = 95\%$ . High RH near 100% indicates potential fog or low clouds.
- $\tau_{\Delta P}$ : Pressure Trend Maximum.  $\tau_{\Delta P} = -1.5$  hPa/hour. A rapid drop indicates rapidly deteriorating weather.
- $\tau_{\text{OCI}}$ : Obstacle Clearance Index Minimum.  $\tau_{\text{OCI}} = 1.0$  m. Minimum required clearance from ultrasonic detection.

The FPV is NO-GO if any of the following conditions are met:

1.  $VIC \leq \tau_{\text{VIC}}$  (Visibility Failure)
2.  $RH \geq \tau_{\text{RH}}$  AND  $T \leq 5^\circ\text{C}$  (Icing/Fog Potential)
3.  $\frac{dP}{dt} \leq \tau_{\Delta P}$  (Rapid Weather Deterioration)
4.  $OCI \leq \tau_{\text{OCI}}$  (Local Obstacle)

The FPV is computed at 1 Hz on the AFN and propagated to adjacent nodes, ensuring continuous path safety validation.

## E References

1. Sharma B. Senior Pilot at Simrik Air Pvt Ltd. Personal communication. 2025.
2. Federal Aviation Administration. Radio Communications Phraseology and Techniques. Available from: [https://www.faa.gov/air\\_traffic/publications/atpubs/aim\\_html/chap4\\_section\\_2.html](https://www.faa.gov/air_traffic/publications/atpubs/aim_html/chap4_section_2.html)

3. Civil Aviation Authority of Nepal. Civil Aviation Regulation, 2058. Available from: [https://nepalindata.com/media/resources/bulkuploaded/Civil-Aviation-Reg-2nd-eng\\_SEP17.pdf](https://nepalindata.com/media/resources/bulkuploaded/Civil-Aviation-Reg-2nd-eng_SEP17.pdf)
4. ICAO. *Annex 10: Aeronautical Telecommunications*. Volume I: Radio Navigation Aids. Montreal: International Civil Aviation Organization.
5. Welsh, B., and B. H. Munk, *A New Method of Estimating Visibility by Combined Optical and Meteorological Sensing*. Applied Optics, 2012.
6. Espressif Systems. *ESP32-S3 Series Datasheet*. 2024.
7. Grewal, M. S., and A. P. Andrews, *Kalman Filtering: Theory and Practice with MATLAB*. John Wiley & Sons, 2015.
8. Perkins, C. E., *Ad Hoc Networking*. Addison-Wesley, 2001.
9. Bosch Sensortec. *BME280 Integrated Environmental Sensor Datasheet*. 2023.
10. Nordic Semiconductor. *nRF24L01+ Single Chip 2.4 GHz Transceiver Datasheet*. 2018.

## F Extended Discussion on Advanced FPV Modeling and Integration

### F.1 Probabilistic Forward Path Viability (PFPV)

While the current FPV model is deterministic (Boolean), future iterations should adopt a probabilistic approach. The PFPV would treat each sensor reading as a random variable with a confidence interval derived from the EKF covariance matrix  $\mathbf{P}$ . The probability of safety  $P(\text{Safe})$  is then defined as the probability that the composite risk function  $F_{\text{safety}}$  exceeds the critical threshold  $\tau_{\text{crit}}$ . This approach provides a continuous risk score instead of a binary output, enhancing pilot decision support.

$$P(\text{Safe}) = P(F_{\text{safety}} > \tau_{\text{crit}}) = 1 - \Phi\left(\frac{\tau_{\text{crit}} - \mu_F}{\sigma_F}\right)$$

Where  $\Phi$  is the Cumulative Distribution Function of the standard normal distribution, and  $\mu_F$  and  $\sigma_F$  are the estimated mean and standard deviation of  $F_{\text{safety}}$  based on the sensor fusion outputs.

### F.2 Thermal and Density Altitude Correction

The performance of rotorcraft is critically dependent on **Density Altitude (DA)**. The AFN, using EKF-corrected altitude  $h_{\text{EKF}}$  and AHT20 temperature  $T$ , computes DA:

$$DA = h_{\text{EKF}} + 118.8 \cdot (T - T_{\text{std}})$$

where  $T_{\text{std}}$  is the standard atmosphere temperature at  $h_{\text{EKF}}$ . This DA value is a critical component of the AFN state vector for dispatch decisions, as it directly impacts engine power available and required rotor pitch.

### F.3 Integration of Image Processing for RVR Estimation

The current luminance sensor (LDR) is a crude proxy for RVR (Runway Visual Range). Future work necessitates the integration of a low-power, wide-angle camera (e.g., OV7670) and on-device **Convolutional Neural Networks (CNNs)** on the ESP32-S3's secondary core. The CNN would be trained on local fog/haze imagery to directly estimate the visual contrast reduction, providing a more accurate RVR equivalent. This would transition the AFN from a simple IoT device to an **Edge-AI** system.

### F.4 Advanced Obstacle Detection with 3D Mapping

The HC-SR04 ultrasonic sensor provides only basic distance measurement. For comprehensive safety, the AFN must be upgraded with a low-power **Solid-State LiDAR** module. This allows the AFN to generate a localized **Point Cloud Map (PCM)** of the helipad surroundings. The DRL would then perform **Conflict Detection and Resolution (CDR)** by analyzing the trajectory of the approaching helicopter (via its transponded GPS) against the static PCM, mitigating the risk of wires, antennae, or other low-visibility obstacles.

## G System Hardening and Reliability Engineering

### G.1 Fault Tolerance and Redundancy Schemes

#### G.1.1 Triple Modular Redundancy (TMR) for Sensors

To enhance reliability, the AFN should transition from single sensors to a Triple Modular Redundancy (TMR) scheme for critical measurements (Baro and LDR). Three independent sensors would be monitored. A **Voting Logic Module (VLM)** would determine the reliable value by discarding the outlier if one sensor deviates by more than  $2\sigma$  from the median of the three.

#### G.1.2 Watchdog Timer and Firmware Robustness

The ESP32-S3's internal **Watchdog Timer (WDT)** is configured to automatically reset the device if the main application loop stalls for more than 500 ms. Furthermore, the firmware is built with **Over-The-Air (OTA) update capability**, allowing remote deployment of bug fixes and algorithm updates to all AFNs via the SN without requiring physical access, a crucial feature for remote mountain deployments.

### G.2 Energy Harvesting and Power Management

Given the remote nature of deployment, AFNs are powered by solar panels and rechargeable Lithium Polymer (LiPo) batteries. The ESP32-S3's **Deep Sleep Mode** is leveraged between data collection cycles to conserve energy.

- **Power Budget:** The system's target average power consumption is 200 mW. The most power-intensive components (nRF24L01+ and GPS) are only powered up for brief intervals (100 ms) for transmission and position acquisition.
- **Solar Sizing:** A 10 W solar panel is required, coupled with a Maximum Power Point Tracking (MPPT) charge controller to ensure consistent battery charging even under low-light (high-altitude haze) conditions.

## H Detailed Discussion on DRL and Graph Theory

### H.1 The Weighted Graph Representation

The HERMES-ATC network is modeled as a directed, weighted graph  $G = (V, E, W_{\text{cost}})$ .

- **Vertices ( $V$ ):** The set of all Autonomous Field Nodes (AFNs) and known, safe alternate landing sites.
- **Edges ( $E$ ):** The potential flight path segments between nodes.
- **Cost Function ( $W_{\text{cost}}$ ):** The weight of an edge  $E_{i \rightarrow j}$  is defined as a cost related to risk and distance:

$$W_{\text{cost}}(i, j) = \alpha_{\text{risk}} \cdot (1/PFPV_{i \rightarrow j}) + \alpha_{\text{dist}} \cdot D_{i \rightarrow j}$$

where  $\alpha_{\text{risk}}$  and  $\alpha_{\text{dist}}$  are regulatory weighting factors,  $PFPV_{i \rightarrow j}$  is the probabilistic forward path viability (Chapter A), and  $D_{i \rightarrow j}$  is the great-circle distance.

## H.2 Dijkstra’s Algorithm Implementation

The DRL utilizes Dijkstra’s algorithm to find the minimum-cost (lowest-risk) path from the current node  $S$  to the destination node  $T$ .

1. **Initialization:** Set the cost to  $S$  as 0 and all other costs to  $\infty$ .
2. **Iteration:** While unvisited nodes remain, select the unvisited node  $u$  with the lowest cost. Mark  $u$  as visited.
3. **Relaxation:** For each neighbor  $v$  of  $u$ , update the cost to  $v$  if the path through  $u$  is cheaper:

$$\text{cost}[v] = \min(\text{cost}[v], \text{cost}[u] + W_{\text{cost}}(u, v))$$

The DRL executes this algorithm on the SN every time a node reports a State C (IMC) condition, providing the most current lowest-risk path for rerouting. The result is a sequence of node IDs that form the recommended diversion route.

## I Security Considerations and Data Integrity

### I.1 Message Authentication Code (MAC)

Given the safety-critical nature of the transmitted guidance, packets must be authenticated to prevent spoofing. The current CRC-16 only verifies data integrity. A lightweight **Message Authentication Code (MAC)** must be implemented using a simple symmetric key, pre-shared among all AFNs and the SN. The MAC ensures that the data originated from a trusted AFN.

### I.2 Physical and Software Security

- **Physical Tamper Resistance:** The remote AFNs must be housed in robust, IP67-rated enclosures, secured with tamper-evident seals to prevent physical attack or manipulation of sensor placement.
- **Firmware Protection:** The ESP32-S3’s flash memory must be encrypted (Flash Encryption) and access to the debug interface (JTAG) disabled to prevent malicious code injection.

## J Future Integration with ADS-B and CAAN Standards

### J.1 ADS-B Integration

The SN’s primary future function is to integrate the AFN data with transponded ADS-B traffic information.

- **Collision Avoidance:** By correlating the helicopter’s projected path (from ADS-B data) with the AFN’s obstacle map (from LiDAR), the SN can compute potential mid-air or terrain conflicts and transmit a warning advisory.
- **Guidance Verification:** The SN can compare the pilot’s execution of the IEGG vectors (derived from the aircraft’s reported GPS position) against the generated ideal vectors, providing post-flight safety analysis.

## J.2 Formal Certification Pathway

Any system intended to influence pilot decisions must undergo a formal certification process. The pathway involves:

1. **Design Assurance Level (DAL) Assignment:** The system is likely to fall under DAL D (No Safety Impact, but related to aviation) or DAL C (Minor Safety Impact, requires formal testing).
2. **Regulatory Documentation:** Creating comprehensive documentation compliant with standards like DO-178C (Software Considerations) and DO-254 (Hardware Considerations).
3. **Real-World Validation:** A phased deployment starting with non-operational advisory service, progressing to simulated operational service, and finally, approved operational use under strict CAAN supervision.

## K Extended Discussion on Environmental Challenges and Adaptation

### K.1 Impact of Low Air Density

In high-altitude environments, the low air density affects both barometric accuracy and the power performance of the nRF24L01+ radios.

- **Barometric Accuracy:** The BME280's accuracy is directly correlated with air density. The EKF must account for a higher process noise covariance (**Q**) at high altitude to reflect this degradation.
- **Radio Performance:** Lower air density can lead to slight changes in the dielectric properties of the environment, potentially affecting RF propagation and antenna matching. The adaptive retransmission logic of the nRF24L01+ compensates for minor signal loss.

### K.2 Monsoon and Extreme Weather Resilience

The system must be engineered to function through the monsoons.

- **Water Ingress:** The IP67 rating ensures protection against rain and dust.
- **Radio Attenuation:** Heavy rainfall introduces significant Rain Fade (attenuation) in the 2.4 GHz band. The HERMES-Routing LQI metric actively monitors for this condition and will switch to a lower-frequency backup communication link (e.g., LoRa) if the 2.4 GHz link becomes persistently unreliable.

This deep dive confirms the feasibility and technical complexity of the HERMES-ATC system.